Multivariate Empirical Modeling of Interaction Effects of Machining Variables on Surface Roughness in Dry Hard Turning of AISI 4140 Steel with Coated CBN Insert Using Taguchi Design

A. CAKAN*, F. EVRENDILEK**

Mersin University, Dep. of Mechanical Engineering, Mersin, Turkey, E-mail: ahcakan@mersin.edu.tr
**Abant Izzet Baysal University, Dep. of Environmental Engineering, Bolu, Turkey, E-mail: fevrendilek@ibu.edu.tr*

1. Introduction

Hard turning is a single point cutting process widely adopted in actual industrial production and concerns the removal of materials whose hardness is higher than 45 HRC. In hard turning, the machining operation is achieved using cutting tool materials purposely developed, such as cubic boron nitride (CBN). CBN presents a unique property combination between hardness/good resistance at high temperature and thermo-chemical stability. These properties are strongly required in cutting tool materials when hard steel parts are machined. The reliability improvements of the CBN cutting tools facilitate the hard turning as a machining process of significant importance in manufacture. Hard turning process enables manufacturers to increase product quality and its efficiency, at the same time to decrease its cost and processing time. This process offers many potential benefits such as high productivity, reduction of cost per product, the ability to machine complex parts by a single setup, reduced setup times, energy conservation, process flexibility, good surface finish, and less environmental pollution without the use of cutting fluid [1-3]. Recently, hard turning of steel parts has become a very popular and effective technology well applied in many areas such as production of bearings, gears, shafts, cams, and other mechanical components. During hard turning, complex and mutual interactions are generated between tool and work piece at the contact surface where significant forces and high temperatures are recorded causing wear and sometimes breakage of the tools [4]. As a result, both the precision of the finished work piece dimension and the surface roughness are altered.

Knowledge about surface finish and tool wear in hard turning process under given cutting variables plays a pivotal role as a dominating criterion of material machinability. To establish a robust functional relationship between such responses as surface roughness and tool wear and such cutting variables as cutting speed, feed rate, depth of cut, nose radius, and cutting time, a large number of tests are needed requiring a separate set of tests for each and every combination of cutting conditions, cutting tool and work piece material. Changes in surface roughness and tool wear during hard turning have been analyzed by many researchers. Aspinwall et al. [5] found that surface roughness had a significant effect on fatigue and other surface properties of the final workpiece. Bouacha et al. [6] quantified surface roughness and cutting force values generated in hard turning with CBN cutting tool. Machining tests are conducted under different cutting conditions, and the cutting variables most influential on surface roughness include feed rate, cutting speed, depth of cut, and cutting force. Lalwani et al. [7] stated that cutting speed had no significant effect on forces and surface roughness; however, feed rate was the primary contributor that significantly influenced the latter. Ozel et al. [8] indicated that, in the finish hard turning of AISI (American Iron and Steel Institute) H13 steel, significant effects of work piece hardness, cutting edge geometry, feed rate and cutting speed on surface roughness. Thiele and Melkote [9] carried out experimental designs to distinguish significant mean differences in surface quality after various runs for finish hard turning using CBN tools. Elbah et al. [10] reported that surface roughness of 4140 steel was improved as cutting speed was elevated and was deteriorated with feed rate when comparing the machinability of hardened AISI 4140 cold work tool steel. Lima et al. [11] pointed out that the surface roughness was improved with increased cutting velocity and was deteriorated with increased feed rate when turning AISI 4340 steel. Benga and Abrao [12] found that feed rate was the most significant factor affecting surface finish and cutting speed had very little influence on surface finish for both ceramic and CBN cutting tool, based on three-level factorial design for machining of hardened 100Cr6 bearing steel (62–64 Rockwell hardness–HRC) using ceramic and CBN tools. El-Wardany et al. [13] experimentally investigated the effect of cutting variables and tool wear on chip morphology and surface integrity during high-speed machining of D2 tool steel (60–62 HRC) using CBN tool. Das et al. [14] determined that feed rate and cutting speed had the most significant effects on changes in surface roughness of hardened alloy steel in the hard machining by using a coated insert tool. Schwach and Guo [15] observed that using a new tool and low feed rate could improve surface roughness and surface integrity of low alloy steel with a hardness of 60 HRC in the turning process.

In the present study, interaction and main effects of cutting variables (cutting speed, and feed rate) under a constant depth of cut on average surface roughness (R_a) and maximum peak-to-valley height (R_z) were quantified in finish hard turning of AISI 4140 low alloy medium carbon steel hardened at HRC 53 ± 1 with CBN inserts. Interaction and main effects of the cutting variables on the surface roughness performance characteristics were explored using Taguchi design. Functional relationship between the cutting variables and performance characteristics was modeled using the best-fit multiple (non-)linear regression—M(N)LR—models.

2. Experimental design

2.1. Workpiece materials

In this experimental study, AISI 4140 high strength medium carbon and low-alloy steel of 60 mm diameter with length of 180 mm were used as the workpiece material. This workpiece material was selected owing to its widespread applications in automotive, crank shafts, rams, spindles, connecting rods, pump, crow bars, ring gears, gear shafts, tie rods and bolts that require high resistance. It contains chromium and molybdenum as alloying elements, and its aptitude for heat treatments allows for meeting most requirements for hardness, strength and ductility. Its chemical composition is thus: 0.38% C; 1.02% Cr; 0.72% Mn; 0.25% Mo; 0.20% Si; 0.030% P; 0.029% S; and balanced Fe.

Initially, the workpiece materials were applied to a heat treatment at 910°C for 30 min and oil quenched. Then, tempering was done at 380°C for 2 h followed by cooling to obtain a homogeneous structure. A standard workpiece hardness of 53 ± 1 HRC was obtained after the heat treatment.

2.2. Cutting inserts

Turning experiments were performed under dry cutting conditions using CBN cutting tool inserts (ISO code CNGA 120408T01030A 7015) manufactured by Sandvik™ Coromant with a thin coating of TiCN layer (1 μm) on the CBN substrate, deposited by the physical vapor deposition (PVD) method. CBN 7015 insert was rigidly mounted on a tool holder with an ISO designation of DCLNR 2525M12 from Sandvik™ Coromant. The combination of the insert and the tool holder resulted in the following geometry: a negative rake angle (γ = -6°), a clearance angle (α = 6°), a negative cutting edge inclination angle (λ = -6°) including angle 80°, and a cutting edge angle (χ_r = 95°) (Fig. 1). These removable inserts are of a square form with four cutting edges whose characteristics are shown in Table 1. For each machining test, a new tool was used.
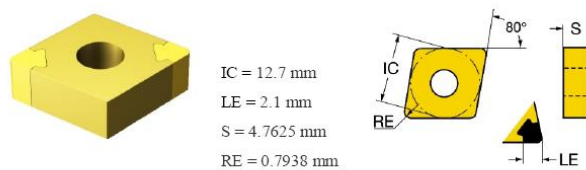

Fig. 1 Cutting tool of CBN 7015 used in this study (S: insert thickness; RE: nose radius; IC: inscribed circle; LE: effective length of cutting edge)

IC = 12.7 mm
LE = 2.1 mm
S = 4.7625 mm
RE = 0.7938 mm

Table 1
Characteristics of inserts used in this study

Cutting materials	Designation	Chemical composition	Hardness (HV)	Thermal conductivity ($Wm^{-1}K^{-1}$)
Cubic boron nitride CBN7015	CNGA120408T01030A	CBN (50%) + ceramic binder	~ 2800	~ 740

2.3. Experimental design of measurements

Hard turning experiments were performed in dry cutting environment on a CNC lathe. The two surface roughness variables of R_a and R_z were measured for each machining condition of individual test using a MarSurf M 300 +RD 18 roughness tester. The measurements of R_a and R_z were performed at various locations of machined work surface, and the average value was taken to evaluate the surface roughness of machined surface. All the surface roughness measurements were obtained directly on the tool machine through disassembling the workpiece by means of a roughness meter. The length examined was 5.60 mm. The measured values of Ra and Rz were within the range 0.922–6.116 μm. The measurements were repeated three times at the three reference lines equally positioned at 120°.

Using the Design Expert 8.0 software (Statease, USA), Taguchi's Orthogonal Array (TOA) design with a full factorial (2^3) was performed to analyze effects of the two cutting variables of cutting speed (V_c) and feed rate (f) under a constant depth of cut (ap = 0.2 mm) on the responses. Table 2 shows the levels of the cutting variables used in hard turning of AISI 4140. The levels of the variables were preferred within the intervals prescribed by cutting tool's manufacture [16].

Table 2
Cutting variables with their levels
used in hard turning experiments

Symbol	Explanatory variable	Unit	Level		
V_c	Cutting speed	m min⁻¹	200	280	
f	Feed rate	mm rev⁻¹	0.04	0.08	0.12

2.4. Statistical analyses

Statistical distribution identification of the response variables was performed evaluating 16 distributions because the normality assumption is primarily of significance to robust inferences for a small sample size (n). Pearson's correlation matrix was carried out to detect direction and strength of significant linear associations among the variables based on correlation coefficient (R) and significance level (P) < 0.05. Multivariate analysis of variance analysis (MANOVA) was performed to compare means of the two simultaneous responses that are highly correlated. Compared to individual ANOVAs, MANOVA has advantages of detecting multivariate response patterns and differences too small to be detected when the response variables are correlated, and minimizing the family error rate (Type I error) equal to selected alpha level (P < 0.05). Tukey's multiple comparison tests following one-way ANOVA were used to detect significant mean differences in the responses in terms of each factor. There are two crossed sources of variability in this experiment: V_c and f. Since each level of f occurs in combination with each level of V_c, these factors are crossed. Fully nested ANOVA was also used to estimate variance components for each response variable. The best-fit multiple (non-)linear regression—M(N)LR—models were built as follows:

$$Ra \text{ or } Rz = \beta + \beta x + ... + \beta x + \varepsilon, \tag{1}$$

where R_a and R_z are the response variables expressed in μm. The terms β_1 to β_n refer to the slope coefficients of the explanatory variables, β_0 is the intercept value, and ε is the residual error. The terms x_1 to x_n refer to explanatory variables which can be of a linear form and/or such non-linear forms

as polynomials through order of up to three, interactions through order of two and/or their combinations. The best-fit M(N)LR model was chosen using the stepwise procedure by which the most significant ones of all 14 possible predictors were retained in the model, based on the alpha-to-enter and alpha-to-remove (P) value of 0.05. All the statistical analyses were performed in Minitab 17 software (Minitab Inc.). Adjusted coefficient of determination (R^2_{adj}), and predicted coefficient of determination (R^2_{pred}) were used to indicate the degree of goodness-of-fit and predictive power, respectively. The values of variance inflation factor (VIF) > 40 were used to indicate the presence of multi collinearity issue, while Durbin-Watson (DW) values were used to indicate no autocorrelation when DW ≈ 2, a strong positive autocorrelation when DW ≈ 0, and a strong negative autocorrelation when DW ≈ 4. The assumptions of Gaussian (nor-mal) distribution of residues, and heteroscedasticity (homogeneity of variance) were tested using Anderson-Darling (AD) normality test, and a plot of residuals versus the predicted values of Y, respectively.

3. Results and discussion

3.1. Linear effects of cutting variables on surface roughness

The experimental response values according to the TAO design are shown in Table 3. Each response variable was fitted with 14 parametric distributions and two transformations which led to the identification of the Johnson transformation, the Box-Cox transformation, and Gaussian distribution as the best-fit distributions for both responses, respectively (Table 4).

Table 3

Mean (± SD) values of surface roughness responses according to the experimental design of Taguchi's orthogonal array (TAO) ($ap = 0.2$ mm; $L_t = 5.60$ mm; $L_c = 0.80$ mm; $n = 3$)

Experimental run	V_c (m min^{-1})	F (mm rev^{-1})	R_a (μm)	R_z (μm)
1	200	0.04	0.922 ± 0.005	4.846 ± 0.02
2	200	0.08	1.063 ± 0.002	5.468 ± 0.008
3	200	0.12	1.131 ± 0.02	5.682 ± 0.04
4	280	0.04	1.076 ± 0.006	5.566 ± 0.03
5	280	0.08	1.123 ± 0.002	5.576 ± 0.01
6	280	0.12	1.192 ± 0.003	6.116 ± 0.01

SD: standard deviation; n: sample size; ap: depth of cut; L_t: traversing length; L_c: cut-off length; V_c: cutting speed; f: feed rate; R_a: average surface roughness; and R_z: maximum peak-to-valley height.

Table 4

Individual distribution identification of response variables ($n = 18$)

Response variable	Distribution parameter	Best-fit distribution		
		Johnson transformation	Box-Cox transformation	Normal
R_a	Location	0.02505	1.5848	1.08439
	Scale	1.32487	0.55175	0.08656
	AD	0.433	0.502	0.874
	P	0.27	0.179	0.02
	λ		5.0	
	Function	0.619685+1.2596×Asinh((x-1.12476)/0.0500528)		
R_z	Location	0.03156	172.57094	5.54244
	Scale	0.86867	34.74672	0.38592
	AD	0.292	0.991	1.091
	P	0.567	0.01	0.005
	λ		3.0	
	Function	0.052501+0.366307×Asinh((x-5.57242)/0.0367168)		

R_a: average surface roughness; R_z: maximum peak-to-valley height. AD: Anderson-Darling statistic; P: significance level; and λ: the optimal lambda value for Box-Cox transformations.

Table 5

Direction, strength and significance of linear relationships among the measured variables based on Pearson's correlation matrix ($n = 18$)

	V_c (m min^{-1})	f (mm rev^{-1})	R_a (μm)
f (mm rev^{-1})	0.0 1.0		
R_a (μm)	0.55 0.01	0.79 0.001	
R_z (μm)	0.56 0.01	0.76 0.001	0.98 0.001

V_c: cutting speed; f: feed rate; R_a: average surface roughness; and R_z: maximum peak-to-valley height.

Person's correlation matrix showed that the response variables had strong and moderate positive correlations with feed rate ($P = 0.001$) and cutting speed ($P = 0.01$), respectively (Table 5). The linear relationship between the response variables resulted in a very high R value of 0.98 ($P = 0.001$). Our MANOVA results indicated that the interaction between feed rate and cutting speed significantly affected the behaviors of the response variables consistently based on all the test statistics of Wilks'lambda ($F = 79.3$; $P = 0.001$), Lawley-Hotelling trace ($F = 132.1$; $P = 0.001$), and Pillai's trace ($F = 46.0$; $P = 0.001$).

3.2. Non-linear effects of cutting variables on surface roughness

Tukey's multiple comparisons following one-way ANOVA show significant mean differences in the response

variables in terms of both interaction effect and main effects (Table 6). This significant interaction implies that the increase in the mean response variables in switching from the low to the high cutting speed depends upon the feed rate. The variance component estimates based on fully nested ANOVA indicated that the variability attributable to cutting speed, and feed rate was 19% ($P > 0.05$) and 80% ($P < 0.001$) for R_a, and was 22% ($P > 0.05$) and 78% ($P < 0.001$) for R_z of the total variability, respectively.

No heteroscedasticity and multicollinearity issues were encountered according to the plot of residuals versus fitted values and the individual VIF values of the model terms, respectively, during the development of the best-fit M(N)LR models (Table 7). The best-fit MNLR model accounted for 96.3% of variation in R_a, while the best-fit MLR model explained 86.9% of variation in R_z (Table 7).

Table 6

Tukey's multiple comparisons following one-way ANOVA and MANOVA results ($n = 3$; $P < 0.001$)

V_c (m min^{-1})	R_a (µm)		R_z (µm)	
	Mean	SE	Mean	SE
200	1.039[b]	0.003	5.332[b]	0.008
280	1.130[a]	0.003	5.753[a]	0.008
f (mm rev^{-1})				
0.04	0.999[b]	0.004	5.206[b]	0.010
0.08	1.093[a]	0.004	5.522[ab]	0.010
0.12	1.161[a]	0.004	5.899[a]	0.010
$V_c \times f$				
200 0.04	0.922[d]	0.005	4.846[e]	0.014
200 0.08	1.063[c]	0.005	5.468[d]	0.014
200 0.12	1.131[b]	0.005	5.682[b]	0.014
280 0.04	1.076[c]	0.005	5.566[c]	0.014
280 0.08	1.123[b]	0.005	5.576[c]	0.014
280 0.12	1.192[a]	0.005	6.116[a]	0.014

V_c: cutting speed; f: feed rate; R_a: average surface roughness; R_z: maximum peak-to-valley height; and SE: standard error

Table 7

The best-fit multiple (non-)linear regression models for R_a ($R^2_{adj} = 96.3\%$; $R^2_{pred} = 95.1\%$; DW = 3; $n = 18$; $P < 0.001$) and R_z ($R^2_{adj} = 86.9\%$; $R^2_{pred} = 83.8\%$; DW = 2.9; $n = 18$; $P < 0.001$)

Response	Model term	Coefficient	SE	VIF
R_a (µm)	Intercept	0.3699	0.063	
	V_c (m min^{-1})	0.0023	0.0002	7
	f (mm rev^{-1})	5.494	0.736	37
	V_c*f	-0.01	0.003	43
R_z (µm)	Intercept	3.586	0.216	
	V_c (m min^{-1})	0.0052	0.0008	1
	f (mm rev^{-1})	8.67	1.0	1

V_c: cutting speed; f: feed rate; R_a: average surface roughness; R_z: maximum peak-to-valley height; SE: standard error; and VIF: variance inflation factor.

The predictive power of the best-fit M(N)LR models was estimated at 95.1% and 83.8% for R_a and R_z, respectively. Based on the best-fit models, the rate of increase in response to the cutting speed and the feed rate was lower in mean R_a than in mean R_z. The rate of increase in mean R_a was estimated at 0.002 µm and 5.49 µm per one-unit increase in V_c (m min^{-1}) and f (mm rev^{-1}), respectively, following the ceteris paribus condition. Similarly, the rate of increase in mean R_z was 0.005 µm and 8.67 µm per one-unit

increase in V_c (m min^{-1}) and f (mm rev^{-1}), respectively (Table 7). In both MNLR and MLR models, the feed rate exerted a greater magnitude of rate of increase than did the cutting speed in the response variables.

The surface roughness-related (R_a and R_z) measurements in response to the cutting conditions are one of the most important requirements in many engineering applications as an important index of product quality. Fig. 2 depicts the interaction effects of feed rate by cutting speed on mean surface roughness properties (R_a and R_z) during hard turning of high strength medium carbon and low-alloy steel using cutting tools. From Fig. 2, it can be clearly seen that mean R_a and R_z values increased with the increased feed rate at different rates depending on the cutting speed and with the increased cutting speed depending on the feed rate. The weaker effect of the cutting speed than the feed rate on the response variables is most likely to result from the increased length of contact between the tool and the workpiece. The interaction plots in Fig. 2 point out to the need to choose both the lowest feed rate and the lowest cutting speed in order to obtain least increases in R_a and R_z values during the machining of hard materials, particularly, AISI 4140. Similar results were reported by Gaitonde et al. [17] and Suresh et al. [18]. Increased cutting speed was reported to produce higher surface roughness similarly by [19, 20].
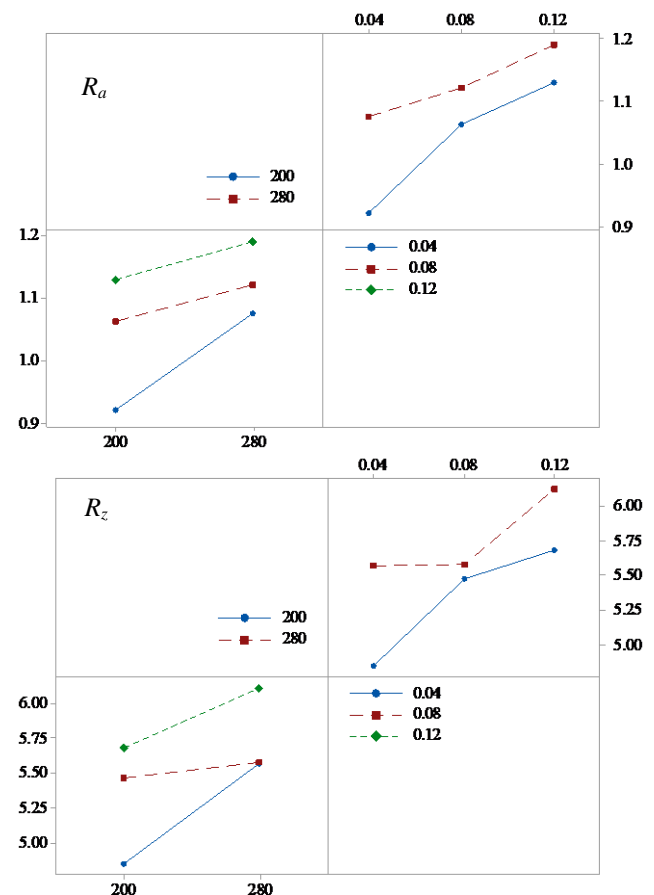

Fig. 2 Rate of change in mean R_a and R_z measured in response to the interactions between the two cutting speeds ($V_c = 200$ and 280 m min^{-1}) and the three feed rates ($f = 0.04$, 0.08 and 0.12 mm rev^{-1}) under a constant depth of cut ($ap = 0.2$ mm).

The minimum mean roughness values of R_a (0.92 $\pm$ 0.005 µm) and R_z (4.84 $\pm$ 0.014 µm) were obtained at the

interaction of the lowest $f = 0.04$ mm rev^{-1} and the lowest $V_c = 200$ m min^{-1}. The maximum mean roughness values of R_a (1.19 $\pm$ 0.005 µm) and R_z (6.11 $\pm$ 0.014 µm) were observed with the interaction of the highest $f = 0.12$ mm rev^{-1} and the highest $V_c = 280$ m min^{-1}. The increased R_a and R_z values with the highest V_c may be attributed to increased nose wear at the high cutting speed. This suggests that increasing nose radius with the lowest feed rate and cutting speed may lead to decreasing surface roughness.

4. Conclusions

The experimental TAO design matrix and its associated results of the surface roughness criteria were analyzed and modeled for cubic boron nitride (CBN7015) inserts during hard turning of AISI 4140 steel. The V_c by f interactions was found to be significant in determining the surface roughness properties of average surface roughness (R_a) and maximum peak-to-valley height (R_z). Feed rate was the most influential factor in the rate and amount of increases in the response variables. Our analyses and modeling results clearly suggests that changes in the surface roughness properties can be minimized employing the lowest levels of the feed rate and the cutting speed in order to ensure an optimal surface roughness value when implementing process optimization. The best-fit M(N)LR models allow for predicting R_a and R_z with the high R^2_{adj} values. The experimental TAO design, and such statistical modeling approaches as (M)ANOVA and M(N)LR proposed in this study appear to be a reliable methodology to optimize and improve the hard turning process and can be extended efficiently to study other machining processes.

Acknowledgement

References

1. **Aouici, H., Bouchelaghem, H.; Yallese, M.A.; Elbah, M., Fnides, B.** 2014. Machinability investigation in hard turning of AISI D3 cold work steel with ceramic tool using response surface methodology, International Journal of Advanced Manufacturing Technology 73: 1775-1788.
http://dx.doi.org/10.1007/s00170-014-5950-0.

2. **Tönshoff, H.K.; Arendt, C.;Amor, B.** 2000. Cutting of hardened steels, TheCIRP Annals-Manufacturing Technology 49: 547-566.
http://dx.doi.org/10.1016/S0007-8506(07)63455-6.

3. **Sahoo, A.K.; Sahoo, B.** 2012. Experimental investigations on machinability aspects in finish hard turning of AISI 4340 steel using uncoated and multilayer coated carbide inserts Measurement 45: 2153-2165.
http://dx.doi.org/10.1016/j.measurement.2012.05.015.

4. **Amara, I.; Ferkous, E.; Bentaleb, F.; Aouad, R.** 2011. The P40 cutting tool wear modelization machining Fk20MnCr5, Engineering 3: 928-934.
http://dx.doi.org/10.4236/eng.2011.39114.

5. **Aspinwall, D.; Dewes, R.; Mantle, A.** 2005. The machining of y-TiAI intermetallic alloys, CIRP Annals-Manufacturing Technology 54: 99-104.

6. **Bouacha, K.; Yallese, M.A.; Mabrouki, T.; Rigal, J.F.** 2010. Statistical analysis of surface roughness and cutting forces using response surface methodology in hard turning of AISI 52100 bearing steel with CBN tool, International Journal of Refractory Metals and Hard Materials 28: 349-361.
http://dx.doi.org/10.1016/j.ijrmhm.2009.11.011.

7. **Lalwani, D.I.; Mehta, N.K.; Jain, P. K.** 2008. Experimental investigations of cutting parameters influence on cutting forces and surface roughness in finish hard turning of MDN250 steel, Journal of Materials Processing Technology 206: 167-179.
http://dx.doi.org/10.1016/j.jmatprotec.2007.12.018.

8. **Özel, T.; Hus, T.K.; Zerne, E.** 2005. Effects of cutting edge geometry, workpiece hardness, feed rate and cutting speed on surface roughness and forces in finish turning of hardened AISI H13 steel, International Journal of Advanced Manufacturing Technology 25: 262-269.
http://dx.doi.org/10.1007/s00170-003-1878-5.

9. **Thiele, J.D.; Melkote, S.N.** 1999. Effect of cutting edge geometry and workpiece hardness on surface generation in the finish hard turning of AISI 52100 steel, Journal of Materials Processing Technology 94: 216-226.
http://dx.doi.org/10.1016/S0924-0136(99)00111-9.

10. **Elbah, M.; Yallese, M.A.; Aouici, H.; Mabrouki, T.; Rigal, J.F.** 2013. Comparative assessment of wiper and conventional ceramic tools on surface roughness in hard turning AISI 4140 steel, Measurement 46(9): 3041-3056.
http://dx.doi.org/10.1016/j.measurement.2013.06.018.

11. **Lima, J.G.; Ávila, R.F.; Abrao, A.M.; Faustino, M.; Davim, J.P.** 2005. Hard turning: AISI 4340 high strength alloy steel and AISI D2 cold work tool steel, Journal of Materials Processing Technology 169(3): 388-395.
http://dx.doi.org/10.1016/j.jmatprotec.2005.04.082.

12. **Benga, G.C.; Abrao, A.M.** 2003. Turning of hardened 100Cr6 bearing steel with ceramic and PCBN cutting tools, Journal of Materials Processing Technology 143-144: 237-241.
http://dx.doi.org/10.1016/S0924-0136(03)00346-7.

13. **El-Wardany, T.I.; Kishawy, H.A.; Elbestawi, M.A.** 2000. Surface integrity of die material in high speed hard machining, Part 1 Micrographical analysis, ASME Journal of Manufacturing Science and Engineering 122: 620-631.
http://dx.doi.org/10.1115/1.1286367.

14. **Das, S.R.; Dhupal, D.; Kumar, A.** 2015. Experimental investigation into machinability of hardened AISI 4140 steel using TiN coated ceramic tool, Measurement 62: 108-126.
http://dx.doi.org/10.1016/j.measurement.2014.11.008.

15. **Schwach, D.W.; Guo, Y.** 2005. Feasibility of producing optimal surface integrity by process design in hard turning, Materials Science and Engineering: A 395: 116-123.
http://dx.doi.org/10.1016/j.msea.2004.12.012.

16. Sandvik coromant Turning tools, Metalworking cutting tools, catalogue, 2013.

17. **Gaitonde, V.N.; Karnik, S.R.; Figueira, L.; Davim, J.P.** 2009. Analysis of machinability during hard turning of cold work tool steel (Type: AISI D2), Journal of Materials Processing Technology 24: 1373-1382.

http://dx.doi.org/10.1080/10426910902997415.

18. **Suresh, R.; Basavarajappa, S.; Samuel, G.L.** 2012. Some studies on hard turning of AISI 4340 steel using multilayer coated carbide tool, Measurement 45(7): 1872-1884.
http://dx.doi.org/10.1016/j.measurement.2012.03.024.

19. **Kim, D.; Ramulu, M.** 2004. Drilling process optimization for graphite/bismaleimide-titanium alloys stacks, Composite Structures 63(1): 101-114.
http://dx.doi.org/10.1016/S0263-8223(03)00137-5.

20. **Kaynak, Y.** 2014. Machining and phase transformation response of room-temperature austenitic NiTi shape memory alloy, Journal of Materials Engineering and Performance 23: 3354.
http://dx.doi.org/10.1007/s11665-014-1058-9.

A. Cakan, F. Evrendilek

MULTIVARIATE EMPIRICAL MODELING OF INTERACTION EFFECTS OF MACHINING VARIABLES ON SURFACE ROUGHNESS IN DRY HARD TURNING OF AISI 4140 STEEL WITH COATED CBN INSERT USING TAGUCHI DESIGN

S u m m a r y

The most important measures of surface quality during the machining process are changes in the average surface roughness and maximum peak-to-valley height caused by such machining variables as cutting speed and feed rate. This study quantifies the interaction effects of the machining variables on surface roughness in dry hard turning process of AISI 4140 steel with CBN7015 inserts. The Taguchi experimental design, (multivariate) analysis of variance, and multiple (non-)linear regression models were combined in the quantification and modeling of interaction effects on surface roughness in dry hard turning process. There existed a significant interaction effect between cutting speed and feed rate in determining the behavior of the response variables.